



## Canadian Journal of Fisheries and Aquatic Sciences

### Epigenetic age estimation in a long-lived, deepwater scorpionfish: insights into epigenetic clock development

Journal:	<i>Canadian Journal of Fisheries and Aquatic Sciences</i>
Manuscript ID	cjfas-2023-0296.R1
Manuscript Type:	Article
Date Submitted by the Author:	24-Jan-2024
Complete List of Authors:	Weber, D. Nick; Texas A&M University-Corpus Christi, Life Sciences Fields, Andrew; Texas A&M University-Corpus Christi, Life Sciences Chamberlin, Derek; University of Florida, Fisheries and Aquatic Sciences; National Marine Fisheries Service, Alaska Fisheries Science Center Patterson, William; University of Florida, Fisheries and Aquatic Sciences Portnoy, David; Texas A&M University-Corpus Christi, Life Sciences
Is the manuscript for consideration in a Special Issue or Collection?:	Not applicable (regular submission)
Keyword:	ageing, DNA methylation, multi-tissue, non-invasive, fish

SCHOLARONE™  
Manuscripts

1 **Epigenetic age estimation in a long-lived, deepwater scorpionfish: insights into epigenetic**  
2 **clock development**

3

4 D. Nick Weber<sup>1\*</sup>, Andrew T. Fields<sup>1</sup>, Derek W. Chamberlin<sup>2,3</sup>, William F. Patterson III<sup>2</sup>, and  
5 David S. Portnoy<sup>1</sup>

6

7 <sup>1</sup> Texas A&M University–Corpus Christi, Department of Life Sciences, 6300 Ocean Drive,  
8 Corpus Christi, TX 78412, USA.

9 <sup>2</sup> University of Florida, School of Forest, Fisheries, and Geomatics Sciences, 7922 NW 71<sup>st</sup>  
10 Street, Gainesville, FL 32653, USA.

11 <sup>3</sup> National Marine Fisheries Service, Alaska Fisheries Science Center, 7600 Sand Point Way  
12 N.E., Building 4, Seattle, WA 98115, USA,

13

14 **\*Corresponding author:** D. Nick Weber (email: [dweber@islander.tamucc.edu](mailto:dweber@islander.tamucc.edu)) and D.S.  
15 Portnoy (email: [david.portnoy@tamucc.edu](mailto:david.portnoy@tamucc.edu)).

16 **Abstract:** Age estimates are essential for fisheries assessment and management, but deepwater  
17 (>200 m) fishes are often difficult to age using traditional techniques. Therefore, age-predictive  
18 epigenetic clocks were developed for a model deepwater reef fish, blackbelly rosefish  
19 *Helicolenus dactylopterus*, using two tissue types (fin clips and muscle; n = 61 individuals; 9–60  
20 years) and  $\Delta^{14}\text{C}$ -validated consensus age estimates. The influence of biological information  
21 (length and sex) on epigenetic clock accuracy, and the potential for developing a multi-tissue  
22 clock, were also assessed. Bisulfite-converted restriction site-associated DNA sequencing  
23 (bsRADseq) was used to identify CpG sites (cytosines followed by guanines) exhibiting age-  
24 correlated DNA methylation, and epigenetic clocks showed strong agreement ( $R^2 > 0.98$ )  
25 between predicted and consensus ages. Including length and sex data enhanced accuracy and  
26 precision ( $R^2 > 0.99$ ; MAE < 1 year). Age-associated CpG sites were identified across tissues,  
27 but a multi-tissue clock performed poorly relative to single-tissue clocks. Overall, results  
28 demonstrate that accurate and precise epigenetic clocks can be developed for deepwater fishes,  
29 and the inclusion of biological information may enhance clock accuracy and precision.

30

31 **Keywords:** ageing, DNA methylation, multi-tissue, non-invasive, fish

## 32 **Introduction**

33 Age estimation provides fish life history information (e.g., age-at-length, age-at-maturity,  
34 age-related fecundity) that is essential for fisheries assessment and management, particularly  
35 when age-structured stock assessment models are used to estimate stock status (Ono et al. 2015).  
36 Techniques used for estimating age typically involve counting growth zones in a range of hard  
37 structures, including otoliths, vertebrae, scales, and fin rays (Campana 2001). Deepwater fishes,  
38 however, are often difficult to age using traditional techniques (e.g., otolith analysis), due largely  
39 to slow growth rates, long life spans, and the constancy of the environment in which they live, all  
40 of which can contribute to difficulty in discerning growth zones (annuli) and higher ageing error  
41 (Cailliet et al. 2001). Thus, the development of an alternative ageing approach would be of great  
42 utility.

43 While other alternative ageing approaches have been explored (e.g., Fourier transform  
44 near infrared spectroscopy, FT-NIRS; Helser et al. 2018; Passerotti et al. 2020), there is  
45 increasing interest in the development of DNA methylation-based, epigenetic ageing techniques  
46 (Piferrer and Anastasiadi 2023). This is due in large part to the fact that epigenetic ageing is  
47 inexpensive relative to otolith-based ageing, non-lethal, and well-suited for rapid age estimation  
48 (Mayne et al. 2023). DNA methylation is an epigenetic mechanism involving a chemical  
49 modification of the DNA, whereby the 5' carbon of cytosine is modified by the addition of a  
50 methyl group (CH<sub>3</sub>; Moore et al. 2013). In vertebrates, DNA methylation typically occurs at  
51 cytosines that are followed by guanines, known as CpG sites, and has been implicated as an  
52 important mechanism for gene regulation (Bommarito and Fry 2019). Recent studies have  
53 demonstrated that changes in DNA methylation levels at certain CpG sites exhibit strong  
54 correlations with chronological age, leading to the development of age-predictive models based

55 on DNA methylation, referred to as epigenetic clocks (reviewed in Parrott and Bertucci 2019 and  
56 Piferrer and Anastasiadi 2023). Epigenetic clocks summarize age-associated increases  
57 (hypermethylation) or decreases (hypomethylation) in DNA methylation across a selected group  
58 of CpG sites throughout the genome, which can be used collectively to estimate chronological  
59 age (Piferrer and Anastasiadi 2023). While the utility of epigenetic age estimation has been  
60 demonstrated in several fish species (European sea bass *Dicentrarchus labrax*, Anastasiadi and  
61 Piferrer 2020; zebrafish *Danio rerio*, Mayne et al. 2020; Australian lungfish *Neoceratodus*  
62 *forsteri*, Murray cod *Maccullochella peelii*, and Mary River cod *Maccullochella mariensis*,  
63 Mayne et al. 2021a; Japanese medaka *Oryzias latipes*, Bertucci et al. 2021; northern red snapper  
64 *Lutjanus campechanus* and red grouper *Epinephelus morio*, Weber et al. 2022; and golden perch  
65 *Macquaria ambigua* spp., Mayne et al. 2023), the application of this ageing technique to a  
66 deepwater fish species has not yet been investigated. The development of epigenetic clocks in  
67 deepwater fishes would seem to be of great utility given the high error often associated with  
68 traditional ageing techniques for deepwater fishes (Cailliet et al. 2001; Campana 2005) and their  
69 vulnerability to overfishing given their longevity and slow growth (Devine et al. 2006).

70 Multi-tissue epigenetic clocks have been developed for mammals (e.g., humans, Horvath  
71 2013; mice, Thompson et al. 2018, and pinnipeds, Robeck et al. 2023), but previously developed  
72 piscine epigenetic clocks have only involved DNA methylation levels identified in a single tissue  
73 type (e.g., fin, Mayne et al. 2020, Mayne et al. 2021a, Weber et al. 2022; muscle, Anastasiadi  
74 and Piferrer 2020, Weber et al. 2022; and liver, Bertucci et al. 2021). While tissue-specific  
75 patterns of DNA methylation have been identified in fishes (Venney et al. 2016; Zupkovitz et al.  
76 2021), the presence of CpG sites exhibiting age-correlated methylation across tissue types (e.g.,  
77 fin clips, muscle), and the potential development of multi-tissue, piscine epigenetic clocks, has

78 not been explored. Fin clips and muscle tissue are commonly sampled during fisheries research,  
79 thus the ability to use a single epigenetic clock for both tissue types may increase the ease with  
80 which age estimates could be obtained, and would also have important implications for future  
81 epigenetic clock development. In addition, the influence of incorporating biological information  
82 (e.g., length and sex) on the development and accuracy of piscine epigenetic clocks remains  
83 unknown (Piferrer and Anastasiadi 2023). Given that length data are often used as a proxy for  
84 age, and that epigenetic regulation plays a major role in sex determination in fishes (Yamagishi  
85 et al. 2022), it is possible that the inclusion of such biological information could enhance  
86 epigenetic clock accuracy and precision.

87         In this study, epigenetic clocks were developed for the blackbelly rosefish (*Helicolenus*  
88 *dactylopterus*), a demersal deepwater scorpionfish that inhabits soft bottom along the continental  
89 shelf and upper slope between 150 and 600 m (Mendonca et al. 2006). The blackbelly rosefish is  
90 widely distributed in the Atlantic Ocean and adjacent seas, including the northern Gulf of  
91 Mexico and Mediterranean Sea, and is commercially targeted in the northeastern Atlantic  
92 (Sequeira et al. 2015). Similar to many other deepwater fishes, blackbelly rosefish exhibit slow  
93 growth ( $k = 0.08 \text{ y}^{-1}$ ) and a long life span (maximum longevity >90 years), which implies low  
94 resilience to fishing pressure (Chamberlin et al. 2023). In addition, like many other deepwater  
95 fishes, blackbelly rosefish are difficult to age by counting growth zones in otoliths. Chamberlin  
96 et al. (2023) recently applied the bomb  $^{14}\text{C}$  chronometer to blackbelly rosefish eye lens cores  
97 (i.e., age-0 metabolic C  $\Delta^{14}\text{C}$  signatures) and validated otolith opaque zone counts (ages 9 to 90  
98 years) as being accurate, overall. However, there was imprecision in ageing between paired  
99 otolith readers. The authors reported an index of average percent error (iAPE) of 4.48% for their

100 study, but 17.50% of their samples were estimated to be >50 years old and the presence of older  
101 ages often depresses iAPE.

102 Study objectives were to: (1) investigate the possibility of developing epigenetic clocks  
103 for the blackbelly rosefish using  $\Delta^{14}\text{C}$ -validated consensus ages, through the *de novo*  
104 identification of CpG sites exhibiting age-correlated DNA methylation; (2) assess the influence  
105 of biological information (i.e., length and sex) on the accuracy of epigenetic clocks; and (3)  
106 assess for the potential development of a multi-tissue epigenetic clock, through the identification  
107 of age-associated CpG sites that are shared across tissue types (fin clips and muscle). The  
108 accuracy and precision of the epigenetic clocks developed were compared to otolith-based  
109 ageing reported by Chamberlin et al. (2023) for the same species.

110

## 111 **Methods**

112 Otoliths and tissue samples were collected from blackbelly rosefish caught between 2020  
113 and 2022 in the northcentral Gulf of Mexico with hook-and-line at depths of 338 to 519 m. Fish  
114 were handled in accordance with the Guide for the Care and Use of Laboratory Animals under  
115 protocols approved by the University of Florida Institutional Animal Care and Use Committee  
116 (Protocol #202111559). Captured fish were measured to the nearest mm fork length and total  
117 length. Otoliths were extracted from fish, rinsed with deionized water, and stored dry in paper  
118 coin envelopes. Eye balls were dissected, placed in plastic bags, and frozen at  $-20\text{ }^{\circ}\text{C}$ .

119 Approximately 4 g of white muscle tissue was dissected from the lateral musculature just below  
120 and in front of the dorsal fin, placed in a plastic bag, and frozen at  $-20\text{ }^{\circ}\text{C}$ . Approximately  $1\text{ cm}^2$   
121 pectoral fin clip samples were removed with scissors, immersed in 20% DMSO-0.25 M EDTA  
122 NaCl-saturated buffer (Seutin et al. 1991), and stored at room temperature until DNA extraction.

123 Fish age was estimated via opaque zone counts in otolith thin sections by two  
 124 independent readers (WFP and DWC), with ageing data originally reported in Chamberlin et al.  
 125 (2023). The index of average percent error (iAPE) was computed between readers for the subset  
 126 of the Chamberlin et al. (2023) samples that were included in epigenetic clock development:

$$127 \quad iAPE = \frac{1}{n} \sum_{j=1}^n \left[ \frac{1}{R} \sum_{i=1}^R \frac{|X_{ij} - X_j|}{\bar{X}_j} \right] \times 100 \quad (\text{Equation 1})$$

128 where  $n$  = number of samples aged;  $R$  = number of age estimates per sample;  $X_{ij}$  is the age  
 129 estimate for the  $i^{th}$  reader's age estimate for the  $j^{th}$  fish ; and  $\bar{X}_j$  is the mean age estimate  
 130 calculated for the  $j^{th}$  fish (Beamish and Fournier 1981). In addition, right eye lenses were cored  
 131 following freeze drying and analyzed for  $\Delta^{14}\text{C}$ , as reported in Chamberlin et al. (2023). Prior to  
 132 epigenetic clock development, consensus age for each sample was developed by WFP and DWC  
 133 after comparison of reader-estimated ages and  $\Delta^{14}\text{C}$ -predicted ages relative to the Bayesian  
 134 spline model fitted by Chamberlin et al. (2023).

135 Genomic DNA was extracted from fin clip and muscle tissue samples using the Mag-  
 136 Bind Blood & Tissue DNA Kit (Omega Bio-tek, Inc., Norcross, USA), and a library was  
 137 prepared for bisulfite-converted restriction site-associated DNA sequencing (bsRADseq),  
 138 following a modified version of the Trucchi et al. (2016) protocol (described in Weber et al.  
 139 2022). Briefly, restriction digests were performed using *Mfe*I-HF, and unique hemi-methylated  
 140 barcoded adaptors were ligated to each sample (Peterson et al. 2012). Samples were then pooled,  
 141 sheared (Covaris M220 Ultrasonicator, Covaris, Inc., Woburn, USA), and size selected using a  
 142 Pippin Prep Size Selection System (Sage Science, Inc., Beverly, USA). The library was then split  
 143 into two portions, and one portion was bisulfite-treated using an EpiTect Plus Bisulfite Kit  
 144 (Qiagen, Hilden, Germany). Bisulfite treatment converts unmethylated cytosines into uracils  
 145 through chemical deamination, and uracils are subsequently replaced by thymines during PCR

146 amplification. This results in predictable base substitutions at all unmethylated cytosines, which  
147 can be identified by comparing sequences from the treated portion to the untreated portion  
148 (Trucchi et al. 2016). The library (including both the treated and untreated portion) was  
149 sequenced across a single lane on an Illumina NovaSeq 6000 (Illumina, Inc., San Diego, USA).  
150 Bisulfite-treated reads were mapped to a reference genome constructed from the untreated reads  
151 using the *dDocent* pipeline (Puritz et al. 2014) with  $c = 0.88$ ,  $K_1 = 2$ , and  $K_2 = 1$ . Mapped reads  
152 were then filtered to retain primary alignments, proper pairs, and those with a mapping quality  
153  $\geq 40$ .

154 CpG sites that could not be successfully genotyped in the untreated portion or that were  
155 identified as potential single nucleotide polymorphisms (SNPs; defined as sites where  $>5\%$  of  
156 total untreated reads across individuals displayed a cytosine to thymine substitution on the  
157 forward strand or guanine to adenine substitution on the reverse strand) were removed from the  
158 dataset. CpG sites were then filtered to retain only sites present in  $\geq 80\%$  of individuals per tissue  
159 type. Percent methylation was estimated as the number of methylated reads divided by the total  
160 number of reads, and per-site 95% confidence intervals were calculated around the estimate for  
161 each individual (Clopper and Pearson 1934). Only those sites with confidence intervals  $< 0.75$  in  
162 at least 80% of individuals were retained, which is roughly equivalent to an average of 30 reads  
163 per site (Weber et al. 2022).

164 To identify all CpG sites exhibiting age-correlated DNA methylation, a Bayesian  
165 framework was used to estimate the parameters of a generalized linear model (GLM) that  
166 included consensus age, tissue type, and sex as fixed factors and individual as a random factor,  
167 using the package *rstanarm* version 2.19.3 (Goodrich et al. 2020). The response variable was the  
168 binomial expression of the number of methylated reads ( $n$ ) and the total number of reads for each

169 sample ( $k$ ) at a given CpG site ( $n/k$ ). GLMs were considered to have converged if the effective  
170 sample size ( $n_{\text{eff}}$ ), was greater than 2,000 and the Gelman-Rubin convergence diagnostic was  
171 less than 1.01 (Lunn et al. 2013; Muth et al. 2018). CpG sites with a 95% credible interval that  
172 did not include zero for the slope of consensus age versus methylation were considered to exhibit  
173 significant age-correlated methylation. For each CpG site that exhibited age-correlated  
174 methylation, individuals with over-dispersed confidence intervals ( $>0.75$ ) were entered as  
175 missing data. Because downstream analysis does not allow for missing data, methylation  
176 frequencies at missing individuals/sites were imputed using the package *mice* version 3.9.0 (van  
177 Buuren and Groothuis-Oudshoorn 2011).

178         The relationship between consensus age and percent methylation across CpG sites was  
179 characterized using elastic net penalized regression modeling, as implemented in the package  
180 *glmnet* version 4.0.2 (Friedman et al. 2010). Independent models were constructed for each  
181 tissue type (i.e., fin clips and muscle) and for both tissue types combined. Given the genomic  
182 approach used (i.e., bsRADseq), and the large number of age-correlated CpG sites identified, the  
183 number of CpG sites included in each of the three models must be reduced prior to penalized  
184 regression modeling. This was accomplished iteratively by evaluating independent Pearson  
185 correlation values (Bertucci et al. 2021), obtained using the ‘corr.test’ function from the package  
186 *psych* version 2.2.9, and model slope coefficients from ‘cv.glmnet’ run with an alpha ( $\alpha$ ) of 0.  
187 For each model, 80% of samples were randomly assigned to a training dataset and the remainder  
188 into a testing dataset, using the ‘partition’ function from the package *splitTools* version 0.3.2  
189 (Mayer 2003). Final predictive models were then constructed using the training datasets and the  
190 ‘cva.glmnet’ function in *glmnet*, which simultaneously cross validates both the penalty and alpha  
191 parameters. Penalized regression modeling (including CpG site reduction) was then repeated

192 with the simultaneous inclusion of fork length and total length, and then performed separately for  
193 males and females. Finally, to determine if an epigenetic clock developed using one tissue type  
194 (e.g., fin clips) could be used to obtain accurate age estimates from another tissue type (e.g.,  
195 muscle), the CpG sites included in the final fin clip model were used to predict age using the  
196 muscle tissue samples, and vice-versa.

197 Model performance for training and testing datasets was assessed using linear regressions  
198 and by comparing mean absolute error (MAE) rates between consensus ages and ages predicted  
199 by the epigenetic clocks. To assess for potential overfitting, Fisher's  $F$ -tests ( $\alpha = 0.05$ ),  
200 conducted using the 'var.test' function from the package *stats* version 3.6.0, were used to  
201 determine if the variance in the residuals differed between training and testing datasets. Relative  
202 error was calculated by dividing the absolute error by the consensus age, and linear regressions  
203 were conducted on consensus age versus relative error in the testing datasets, to determine if  
204 error in the models increased with increasing age. Lastly, iAPE was computed between  
205 consensus ages and predicted ages for all epigenetic clocks (Equation 1). All analyses were  
206 conducted in *R* version 3.6.0 (R Core Team 2023).

207

## 208 **Results**

### 209 *Sampling and age estimation*

210 In total, 61 blackbelly rosefish were sampled for otoliths and tissues, with fin clip and  
211 muscle tissue samples available for 32 individuals, fin clips only from 24 individuals, and muscle  
212 tissue only from 5 individuals. Otolith sections (Fig. 1) were produced for these samples and  
213 paired age estimates (readers: WFP and DWC) analyzed and reported in Chamberlin et al.  
214 (2023). The overall index of average percent error (iAPE) between readers reported for

215 blackbelly rosefish ( $n = 356$ ) aged in Chamberlin et al. (2023) was 4.48% for fish that ranged in  
216 age from 9 to 90 years. Recomputing the iAPE for the subset of samples ( $n = 61$ ) analyzed herein  
217 for epigenetic clock development produced an estimate of 6.47%. Consensus ages among these  
218 samples ranged from 9 to 60 years (Supp. Data<sup>1</sup>).

219

### 220 *Epigenetic clock development*

221 Across all individuals ( $n = 61$ ) and both tissue types, 2,959,164 CpG sites were  
222 recovered. A total of 175,973 sites either could not be successfully genotyped in the untreated  
223 portion of the library or were identified as potential SNPs and removed from the dataset.

224 Across all fin clips ( $n = 56$ ), 156,529 CpG sites had sufficiently tight confidence intervals  
225 in at least 80% of individuals. Mean ( $\pm$  SD) global CpG methylation was 85.20% ( $\pm$  0.91%).  
226 Bayesian GLMs identified 10,139 CpG sites that exhibited significant age-correlated  
227 methylation, and penalized regression analysis retained 316 CpG sites in the age-predictive  
228 model. Strong agreement was observed between consensus age and predicted age in both the  
229 training ( $R^2 = 0.98$ ) and testing ( $R^2 = 0.98$ ) datasets (Fig. 2A,B; Table 1). Mean absolute error  
230 (MAE) was 1.66 and 1.62 years in the training and testing datasets, respectively (Fig. 2A,B;  
231 Table 1). Variance in the residuals did not differ between training and testing datasets (Fisher's  
232  $F$ -test,  $p = 0.81$ ), and relative error in the testing dataset did not increase with increasing age ( $p =$   
233 0.35;  $R^2 = 0.09$ ).

234 Across all muscle tissue samples ( $n = 37$ ), 115,569 CpG sites had sufficiently tight  
235 confidence intervals in at least 80% of individuals. Mean ( $\pm$  SD) global CpG methylation was  
236 85.40% ( $\pm$  0.45%). Bayesian GLMs identified 5,886 CpG sites that exhibited significant age-

---

<sup>1</sup>Supplementary data are available with the article at XXX.

237 correlated methylation, and penalized regression analysis retained 312 CpG sites in the age-  
238 predictive model. As above for the fin clip samples, strong agreement was observed between  
239 consensus age and predicted age in both the training ( $R^2 = 0.99$ ) and testing ( $R^2 = 0.98$ ) datasets  
240 (Fig. 2C,D; Table 1). MAE was 2.07 and 2.14 years in the training and testing datasets,  
241 respectively (Fig. 2C,D; Table 1). Variance in the residuals did not differ between training and  
242 testing datasets (Fisher's  $F$ -test,  $p = 0.70$ ), and relative error in the testing dataset did not  
243 increase with increasing age ( $p = 0.66$ ;  $R^2 = 0.03$ ).

244

#### 245 *Influence of biological information*

246 The inclusion of length data (fork length and total length) enhanced the accuracy and  
247 precision of the fin clip clock ( $R^2 = 0.99$  and MAE = 0.90 years in the testing dataset; Fig. 3B;  
248 Table 2) and the muscle tissue clock ( $R^2 = 0.99$  and MAE = 1.25 years in the testing dataset; Fig.  
249 3D; Table 2). Including sex data and performing the same analysis separately for males and  
250 females further enhanced the accuracy and precision of both the fin clip clock ( $R^2 = 0.99$ , MAE =  
251 0.43 years for males and  $R^2 = 0.99$ , MAE = 0.42 years for females in the testing dataset; Fig. 4B;  
252 Table 2) and the muscle tissue clock ( $R^2 = 0.99$ , MAE = 0.78 years for males and  $R^2 = 0.99$ ,  
253 MAE = 0.80 years for females in the testing dataset; Fig. 4D; Table 2).

254

#### 255 *Multi-tissue epigenetic clock development*

256 Across both tissue types ( $n = 56$  fin clips;  $n = 37$  muscle tissue), 129,916 CpG sites had  
257 sufficiently tight confidence intervals in at least 80% of individuals. Mean ( $\pm$  SD) global CpG  
258 methylation was 85.20% ( $\pm 0.78\%$ ). Bayesian GLMs identified 5,063 CpG sites that exhibited  
259 significant age-correlated methylation, and no significant difference in methylation between

260 tissue types. For modeling purposes, however, all 15,953 CpG sites that exhibited a significant  
261 relationship with age, regardless of significant relationships with tissue type or their interaction  
262 in the Bayesian GLM, were included. Penalized regression analysis retained 498 CpG sites in the  
263 age-predictive model. The multi-tissue clock performed relatively well for the fin clip samples  
264 ( $R^2 = 0.94$  and MAE = 3.08 years in the testing dataset; Fig 5B; Table 1), but not for the muscle  
265 tissue samples ( $R^2 = 0.77$  and MAE = 5.43 years in the testing dataset; Fig. 5B; Table 1).  
266 Variance in the residuals did not differ between the training and testing datasets for either tissue  
267 type (Fisher's  $F$ -tests; fin clips,  $p = 0.83$ ; muscle tissue,  $p = 0.58$ ). Forty-four of the 498 CpG  
268 sites included in the multi-tissue clock were also included in the fin clip clock, and 21 of the 498  
269 CpG sites included in the multi-tissue clock were included in the muscle tissue clock.

270 The epigenetic clock developed using the fin clip samples ( $n = 316$  CpG sites) was  
271 unable to accurately predict the ages of the muscle tissue samples ( $R^2 = 0.10$ , MAE = 13.30  
272 years; Fig. S1A). Similarly, the epigenetic clock developed using the muscle tissue samples ( $n =$   
273 312 CpG sites) was unable to accurately predict the ages of the fin clip samples ( $R^2 = 0.18$ , MAE  
274 = 12.19 years; Fig. S1B).

275

#### 276 *Epigenetic clock index of average percent error*

277 The iAPE for epigenetic clocks developed using fin clips ranged from 1.04% to 2.77%  
278 for testing datasets and 2.95% to 4.46% for training datasets (Table 3). Among muscle tissue  
279 epigenetic clocks, iAPE ranged from 1.45% to 4.31% for testing datasets and 2.67% and 5.23%  
280 for training datasets (Table 3). The iAPE for all epigenetic clocks was lower than the iAPE  
281 computed between otolith readers (6.47%) for the individuals analyzed herein ( $n = 61$ ).

282

## 283 **Discussion**

284           The development of accurate and precise epigenetic clocks for the blackbelly rosefish  
285 suggests epigenetic clocks could provide a non-lethal, efficient, and effective ageing approach  
286 for deepwater fishes that are difficult to age using traditional ageing techniques. The high  
287 accuracy and precision reported are particularly important in the context of fisheries assessment  
288 and management, given that error in age estimation propagates as bias or imprecision in the  
289 estimation of population parameters (e.g., growth, mortality, yield per recruit) and stock  
290 assessment outputs (Lai and Gunderson 1987). In addition, while the demand for fish ageing is  
291 increasing, otolith ageing is a time- and cost-intensive process, often limiting the amount of data  
292 that can be collected and incorporated into stock assessments (Helser et al. 2019). The results  
293 presented herein contribute to a growing body of literature demonstrating the potential for  
294 epigenetic ageing to greatly impact the way in which age estimates are generated and the volume  
295 of data available for stock assessments.

296           Single-tissue epigenetic clocks developed here were both accurate and precise, with  
297 greater levels of precision than reported for ageing of blackbelly rosefish using traditional annuli  
298 counts in otoliths (Chamberlin et al. 2023). While the epigenetic clock developed using the fin  
299 clips appeared to perform better than the clock developed using muscle tissue, this result is likely  
300 due in part to the smaller sample size for muscle tissue than fin clips ( $n = 37$  and  $n = 56$ ,  
301 respectively). The accuracy and precision of epigenetic clocks are likely attributable to a variety  
302 of factors, including the number of individuals incorporated, the age range of those individuals,  
303 the accuracy of the age estimates used to train the clock, the number of age-correlated CpG sites  
304 evaluated, and the degree of environmental influence on the epigenome of the species of interest.  
305 A recent simulation study indicated that a minimum sample size of 70 individuals in the training

306 dataset is necessary to maximize epigenetic clock accuracy and precision (Mayne et al. 2021b),  
307 and while that study could not account for all of the factors listed above, results of the present  
308 study are consistent with that guidance, as the clock developed with the larger training dataset  
309 (fin clip) performed better than the clock developed with the smaller training dataset (muscle  
310 tissue). Having said that, among the 51 tissues and cell types included in the human epigenetic  
311 clock, skeletal muscle tissue was among the poorer predictors of age (Horvath 2013). Therefore,  
312 a biological basis for the decreased accuracy observed in the muscle tissue clock (e.g., plasticity,  
313 high stem cell content) cannot be ruled out.

314 Notably, model performance did not decrease with increasing age in the fin clip or  
315 muscle tissue clocks, which is contrary to results from previous studies that utilized  
316 evolutionarily conserved age-associated DNA methylation at CpG sites identified in the  
317 zebrafish (*Danio rerio*, e.g., Mayne et al. 2021a; Mayne et al. 2023). This is particularly  
318 important for long-lived species like the blackbelly rosefish, and is likely the result of  
319 characterizing a large number of independent CpG sites exhibiting age-correlated methylation  
320 specifically within the blackbelly rosefish genome and across individuals exhibiting a wide age  
321 range. Moreover, the use of consensus otolith-derived age estimates, validated via application of  
322 the bomb radiocarbon chronometer (Chamberlin et al. 2023), to train the epigenetic clocks likely  
323 contributed to the observed accuracy and precision. Thus, when maximizing accuracy is the  
324 primary focus, it is important to consider the potential benefits of developing epigenetic clocks  
325 *de novo* in the species of interest.

326 The inclusion of biological information (i.e., length and sex data) enhanced the accuracy  
327 and precision of the fin clip and muscle tissue clocks. Length data can be easily and non-  
328 invasively collected and could thus be included in epigenetic-based age estimation with minimal

329 effort. The epigenetic clocks developed with length data also required fewer CpG sites to predict  
330 age, which is important to consider when generating assays for production ageing (i.e., the  
331 efficient generation of age estimates for large numbers of individuals needed for fisheries  
332 assessment; Passerotti et al. 2020), such as via genotyping-in-thousands by sequencing (GT-seq;  
333 Campbell et al. 2015), because PCR assays are easier to design with fewer loci. While  
334 Anastasiadi and Piferrer (2020) reported that the inclusion of length data did not have an effect  
335 on epigenetic age estimation in the European sea bass (*Dicentrarchus labrax*), this difference  
336 may be due to the fact that length data were treated as a covariate in a regression of predicted age  
337 versus chronological age in that study, while length data were treated as predictor variables  
338 during epigenetic clock development in the present study. The accuracy and precision of the  
339 epigenetic clocks further improved when males and females were modeled separately, suggesting  
340 patterns of age-associated DNA methylation are somewhat sex-specific. This is supported by  
341 previous research conducted on humans (reviewed in Yusipov et al. 2020) and roe deer  
342 (*Capreolus capreolus*, Lemaitre et al. 2022), where distinct patterns in epigenetic ageing were  
343 identified between sexes. Because many teleost species of commercial interest exhibit large  
344 differences in growth rate and maximum size between sexes (e.g., Atlantic cod *Gadus morhua*  
345 and Pacific halibut *Hippoglossus stenolepis*, Pifferer and Anastasiadi 2023), it is possible that the  
346 design of sex-specific epigenetic clocks will be necessary to maximize accuracy and precision.  
347 While sex data are routinely and non-invasively collected for species displaying sexual  
348 dimorphisms (e.g., elasmobranchs and some teleosts, including mahi mahi *Coryphaena hippurus*  
349 and black rockfish *Sebastes melanops*), sex data can also be non-invasively obtained via genetic  
350 methods (e.g., genotyping sex-specific markers; Bargen et al. 2015) for species with genetic sex

351 determination. Thus, the inclusion of sex-specific markers in epigenetic clock panels could allow  
352 for the determination of both age and sex via the same tissue sample.

353 A number of CpG sites exhibiting age-correlated DNA methylation were shared between  
354 fin clip and muscle tissue samples, allowing for the development of a multi-tissue piscine  
355 epigenetic clock. However, the relatively poor performance of the multi-tissue clock, when  
356 compared to the clocks built separately for fin clips and muscle tissue, suggests age-related  
357 changes in DNA methylation may be tissue-specific. This is supported by the fact that no CpG  
358 sites were shared between the fin clip and muscle tissue clocks developed herein, and further  
359 supported by the fact that the epigenetic clocks developed using one tissue type (e.g., fin clips)  
360 were unable to accurately predict the ages of the other tissue type (e.g., muscle tissue). This is  
361 consistent with results from previous studies conducted on humans (Horvath 2013; Christensen  
362 et al. 2009), rats (Thompson et al. 2010), mice (Thompson et al. 2018), and common bottlenose  
363 dolphins (Robeck et al. 2021a), all of which demonstrated tissue-specific age-related changes in  
364 DNA methylation. Thus, while the identification of age-associated CpG sites shared between  
365 tissue types allowed for the development of a multi-tissue clock, the simultaneous development  
366 of tissue-specific clocks likely requires similar time and effort, and the results presented herein  
367 support the notion that single-tissue epigenetic clocks are generally more accurate than multi-  
368 tissue clocks (Robeck et al. 2021b).

369 Age estimates for all muscle tissue samples from individuals >50 years old were  
370 underpredicted in the multi-tissue clock, while all but one fin clip sample from individuals >50  
371 years old were overpredicted, suggesting the presence of tissue-specific differences in ‘tick rates’  
372 (i.e., the rates of change in DNA methylation). While tissue-specific differences in tick rates  
373 have not been documented in fishes (Piferrer and Anastasiadi 2023), this phenomenon is well

374 established in humans (Horvath and Raj 2018). The use of skeletal muscle tissue led to the  
375 underprediction of age in a multi-tissue epigenetic clock developed for humans, perhaps due to  
376 the rejuvenation of DNA methylation profiles in muscle tissue via myosatellite cells – muscle  
377 stem cells involved in muscle growth and regeneration following injury or disease (Horvath  
378 2013). Recognizing that tissue-specific differences in tick rates may exist in fishes, caution  
379 should be taken against building epigenetic clocks with tissues prone to epigenetic age  
380 acceleration (i.e., higher tick rates; e.g., kidney, brain; Piferrer and Anastasiadi, 2023).

381 Overall, the present study adds to the growing body of literature on the development and  
382 application of epigenetic clocks for fishes (reviewed in Anastasiadi and Pifferer 2023 and  
383 Piferrer and Anastasiadi 2023). The results presented for blackbelly rosefish demonstrate that  
384 accurate and precise epigenetic clocks can be developed for long-lived, deepwater fish species,  
385 which are often vulnerable to overfishing (Devine et al. 2006) and difficult to age using  
386 traditional techniques (Campana 2005; Kestelle et al. 2020). In addition, this study demonstrates  
387 the inclusion of biological information (i.e., length and sex), which is commonly available and  
388 easily and nondestructively obtained, can improve clock performance. Finally, while the ability  
389 to develop a multi-tissue piscine clock was demonstrated herein, the results suggest age-related  
390 changes in DNA methylation are tissue-specific and single-tissue epigenetic clocks may provide  
391 higher accuracy than multi-tissue clocks. When compared to traditional ageing techniques (e.g.,  
392 otolith analysis), the use of epigenetic clocks to obtain age estimates is relatively inexpensive  
393 (Mayne et al. 2021a), non-lethal, and not hindered by between-reader precision issues. Thus,  
394 while epigenetic clocks have the potential to greatly advance the generation of age estimates for  
395 fisheries research and management, continued research on the best practices to enhance clock  
396 accuracy and precision (e.g., using validated age estimates to train models, incorporating

397 biological information, the choice of tissue type, species-specific versus multi-species clocks,  
398 and more sophisticated modeling approaches) is warranted.

399

#### 400 **Acknowledgements**

401 We thank all individuals who assisted with sample collection, including Joe Tarnecki,  
402 Miaya Taylor, Captain Johnny Green, and the crew of the F/V Intimidator. We also thank Kathy  
403 Elder, Susan Handwork, and the NOSAMS staff for eye lens  $\Delta^{14}\text{C}$  analysis. This is publication  
404 37 of the Marine Genomics Laboratory and 129 of Genetic Studies in Fishes (Genetic Studies in  
405 Marine Fishes).

406

#### 407 **Competing interests statement**

408 The authors declare there are no competing interests.

409

#### 410 **Author contribution statement**

411 **DNW:** conceptualization, data curation, methodology, formal analysis, writing – original  
412 draft; **ATF:** conceptualization, methodology, formal analysis, writing – review and editing;  
413 **DWC:** data curation, writing – review and editing; **WFP:** conceptualization, data curation,  
414 supervision, funding acquisition, writing – review and editing; **DSP:** conceptualization,  
415 methodology, resources, supervision, funding acquisition, writing – review and editing.

416

#### 417 **Funding statement**

418 This work was supported by a NMFS-Sea Grant Joint Fellowship in Population and  
419 Ecosystem Dynamics (No. NA20OAR417066) from the National Marine Fisheries Service and

420 the National Sea Grant College Program, and a “Grant-In-Aid” from the Texas Sea Grant  
421 “Grants-In-Aid” of Graduate Research Program. Funding for sample collection, otolith ageing,  
422 and eye lens  $\Delta^{14}\text{C}$  was provided by the NOAA Fisheries Cooperative Research Program (No.  
423 NA18NMF4540080), the NOAA Fisheries Marine Fisheries Initiative (No.  
424 NA21NMF4330501), and the University of Florida.

425

#### 426 **Data availability statement**

427 Datasets (raw and filtered) and data analysis scripts are available at  
428 [https://github.com/marinegenomicslab/BBRF\\_EpigeneticAgeing](https://github.com/marinegenomicslab/BBRF_EpigeneticAgeing). Raw bsRADseq sequences will  
429 be made publicly available at the conclusion of a separate ongoing study.

430

#### 431 **References**

- 432 Anastasiadi, D., and Piferrer, F. 2020. A clockwork fish: Age prediction using DNA  
433 methylation-based biomarkers in the European seabass. *Mol. Ecol. Resour.* **20**: 387–397.
- 434 Anastasiadi, D., and Piferrer, F. 2023. Bioinformatic analysis for age prediction using epigenetic  
435 clocks: application to fisheries management and conservation biology. *Front. Mar. Sci.*  
436 **10**: 1096909.
- 437 Bargaen, J.V., Smith, C.T., and Rueth, J. 2015. Development of a Chinook salmon sex  
438 identification SNP assay based on the growth hormone pseudogene. *J. Fish Wildl.*  
439 *Manag.* **6**(1): 213–219.
- 440 Beamish, R.J., and Fournier, D.A. 1981. A method for comparing the precision of a set of age  
441 determinations. *Can. J. Fish. Aquat. Sci.* **38**: 982–983.

- 442 Bertucci, E.M., Mason, M.W., Rhodes, O.E., and Parrot, B.J. 2021. Exposure to ionizing  
443 radiation disrupts normal epigenetic aging in Japanese medaka. *Aging*. **13**: 22752–22771.
- 444 Bommarito, P.A., and Fry, R.C. 2019. The role of DNA methylation in gene regulation.  
445 *Toxicoepigenetics*. Chapter 2-1, pp. 127–151.
- 446 Campana, S.E. 2001. Accuracy, precision and quality control in age determination, including a  
447 review of the use and abuse of age validation methods. *J. Fish. Biol.* **59**: 197–242.
- 448 Campana, S.E. 2005. Otolith science entering the 21<sup>st</sup> century. *Mar. Freshw. Res.* **56**: 485–495.
- 449 Campbell, N.R., Harmon, S.A., and Narum, S.R. 2015. Genotyping-in-thousands by sequencing  
450 (GT-seq): A cost effective SNP genotyping method based on custom amplicon  
451 sequencing. *Mol. Ecol. Resour.* **15**: 855–867.
- 452 Cailliet, G.M., Andrews, A.H., Burton, E.J., Watters, D.L., Kline, D.E., and Ferry-Graham, L.E.  
453 2001. Age determination and validation studies of marine fishes: do deep-dwellers live  
454 longer? *Exp. Gerontol.* **36**: 739–764.
- 455 Chamberlin, D.W., Siders, Z.A., Barnett, B.K., and Patterson III, W.F. 2023. Eye lens-derived  
456  $\Delta^{14}\text{C}$  signatures validate extreme longevity in the deepwater blackbelly rosefish,  
457 *Helicolenus dactylopterus*. *Sci. Rep.* **13**: 7438.
- 458 Christensen, B.C., Houseman, E.A., Marsit, C.J., Zheng, S., Wrensch, M.R., Wiemels, J.L.,  
459 Nelson, H.H., Karagas, M.R., Padbury, J.F., Bueno, R., Sugarbaker, D.J., Yeh, R.,  
460 Wiencke, J.K., and Kelsey, K.T. 2009. Aging and environmental exposures alter tissue-  
461 specific DNA methylation dependent upon CpG island context. *PLoS Genet.* **5**(8):  
462 e:1000602.
- 463 Clopper, C.J., and Pearson, E.S. 1934. The use of confidence or fiducial limits illustrated in the  
464 case of the binomial. *Biometrika.* **26**(4): 404–413.

- 465 Devine, J.A, Baker, K.D., and Haedrich, R.L. 2006. Deep-sea fishes qualify as endangered. Nat.  
466 Commun. **439**: 29.
- 467 Friedman, J., Hastie, T., and Tibshirani, R. 2010. Regularization paths for generalized linear  
468 models via coordinate descent. J. Stat. Softw. **33**(1): 1–22.
- 469 Goodrich, B., Gabry, J., Ali, I., and Brilleman, S. 2020. rstanarm: Bayesian applied regression  
470 modeling via Stan. R package version 2.19.3.
- 471 Helser, T.E., Benson, I., Erickson, J., Healy, J. Kastle, C., and Short, J.A. 2018. A  
472 transformative approach to ageing fish otoliths using Fourier transform near infrared  
473 spectroscopy: a case study of eastern Bering Sea walleye pollock (*Gadus*  
474 *chalcogrammus*). Can. J. Fish. Aquat. Sci. **76**(5): 780–789.
- 475 Helser, T.E., Benson, I.M., and Barnett, B.K. 2019. Proceedings of the research workshop on the  
476 rapid estimation of fish age using Fourier transform near infrared spectroscopy (FT-  
477 NIRS). AFSC Processed Rep. 2019-06. Alaska Fisheries Science Center, NOAA,  
478 National Marine Fisheries Service.
- 479 Horvath, S. 2013. DNA methylation age of human tissues and cell types. Genome Biol. **14**:  
480 R115.
- 481 Horvath, S. and Raj, K. 2018. DNA methylation-based biomarkers and the epigenetic clock  
482 theory of ageing. Nat. Rev. **19**: 371–384.
- 483 Kastle C.R., Helser, T.E., TenBrick, T., Hutchinson, C., Goetz, B., Gburski, C., and Benson, I.  
484 2020. Age validation of four rockfishes (genera *Sebastes* and *Sebastolobus*) with bomb  
485 <sup>14</sup>C. Mar. Freshw. Res. **71**: 1355–1366.

- 486 Lai, H.L., and Gunderson, D.R. 1987. Effects of ageing errors on estimates of growth, mortality,  
487 and yield per recruit for walleye pollock (*Theragra chalcogramma*). *Fish. Res.* **5**:  
488 287–302.
- 489 Lemaitre, J., Rey, B., Gaillard, J., Regis, C., Gilot-Fromont, E., Debias, F., Duhayer, J.,  
490 Pardonnet, S., Pellerin, M., Haghani, A., Zoller, J.A., Li, C.Z., and Horvath, S. 2022.  
491 DNA methylation as a tool to explore ageing in wild roe deer populations. *Mol. Ecol.*  
492 *Resour.* **22**: 1002–1015.
- 493 Lunn, D., Barrett, J., Sweeting, M., and Thompson, S. 2013. Fully Bayesian hierarchical  
494 modeling in two stages, with application to meta-analysis. *J. R. Stat. Soc. Ser. C Appl.*  
495 *Stat.* **62**(4): 551–572.
- 496 Mayer, M. 2023. splitTools: tools for data splitting. R package version 0.3.2.
- 497 Mayne, B., Korbie, D., Kenchington, L., Ezzy, B., Berry, O., and Jarman, S. 2020. A DNA  
498 methylation age predictor for zebrafish. *Aging.* **12**: 24817–24835.
- 499 Mayne, B., Espinoza, T., Roberts, D., Butler, G.L., Brooks, S., Korbie, D., and Jarman, S. 2021a.  
500 Nonlethal age estimation of three threatened fish species using DNA methylation:  
501 Australian lungfish, Murray cod and Mary River cod. *Mol. Ecol. Resour.* **21**: 2324–2332.
- 502 Mayne, B., Berry, O., and Jarman, S.N. 2021b. Optimal sample size for calibrating DNA  
503 methylation age estimators. *Mol. Ecol. Resour.* **21**: 2316–2323.
- 504 Mayne, B., Espinoza, T., Crook, D.A., Anderson, C., Korbie, D., Marshall, J.C., Kennard, M.J.,  
505 Harding, D.J., Butler, G.L., Roberts, B., Whiley, J., and Marshall, S. 2023. Accurate,  
506 non-destructive, and high-throughput age estimation for Golden perch (*Macquaria*  
507 *ambigua* spp.) using DNA methylation. *Sci. Rep.* **13**: 9547.

- 508 Mendonca, A., Isidro, E., Menezes, G., Pinho, M.R., Melo, O., and Estacio, S. 2006. New  
509 contribution to the reproductive features of bluemouth *Helicolenus dactylopterus* from  
510 the northeast Atlantic (Azores archipelago). *Sci. Mar.* **70**: 679–688.
- 511 Moore, L.D., Le, T., and Fan, G. 2013. DNA methylation and its basic function.  
512 *Neuropsychopharmacology.* **38**: 23–38.
- 513 Muth, C., Oravecz, Z., and Gabry, J. 2018. User-friendly Bayesian regression modelling: a  
514 tutorial with rstanarm and shinystan. *Quant. Meth. Psychol.* **14**(2): 99–119.
- 515 Ono, K., Licandeo, R., Muradian, M.L., Cunningham, C.J., Anderson, S.C., Hurtado-Ferro, F.,  
516 Johnson, K.F., McGilliard, C.R., Monnahan, C.C., Szuwalski, C.S., Valero, J.L., Vert-  
517 Pre, K.A., Whitten, A.R., and Punt, A.E. 2015. The importance of length and age  
518 composition data in statistical age-structured models for marine species. *ICES J. Mar.*  
519 *Sci.* **72**(1): 31–43.
- 520 Parrott, B.B., and Bertucci, E.M. 2019. Epigenetic aging clocks in ecology and evolution. *Trends*  
521 *Ecol. Evol.* **34**: 767–770.
- 522 Passerotti, M.S., Helser, T.E., Benson, I.M., Barnett, B.K., Ballenger, J.C., Buble, W.J.,  
523 Reichert, M.J.M., and Quattro, J.M. 2020. Age estimation of red snapper (*Lutjanus*  
524 *campechanus*) using FT-NIR spectroscopy: feasibility of application to production ageing  
525 for management. *ICES J. Mar. Sci.* **77**(6): 2144–2156.
- 526 Peterson, B.K., Weber, J.N., Kay, E.H., Fisher, H.S., and Hoekstra, H.E. 2012. Double digest  
527 RADseq: an inexpensive method for *de novo* SNP discovery and genotyping in model  
528 and non-model species. *PLoS ONE.* **7**(5): e37135.

- 529 Piferrer, F., and Anastasiadi, D. 2023. Age estimation in fishes using epigenetic clocks:  
530 Applications to fisheries management and conservation biology. *Front. Mar. Sci.* doi:  
531 10.3389/fmars.2023.1062151.
- 532 Puritz, J.B., Hollenbeck, C.M., and Gold, J.R. 2014. dDocent: a RADseq, variant-calling pipeline  
533 designed for population genomics of non-model organisms. *PeerJ*. doi:10.7717/peerj.431.
- 534 Robeck, T.R., Fei, Z., Haghani, A., Zoller, J.A., Li, C.Z., Steinman, K.J., DiRocco, S., Staggs, L.,  
535 Schmitt, T., Osborn, S., Montano, G., Rodriguez, M., and Horvath, S. 2021a. Multi-tissue  
536 methylation clocks for age and sex estimation in the common bottlenose dolphin. *Front.*  
537 *Mar. Sci.* **8**: 713373.
- 538 Robeck, T.R., Fei, Z., Lu, A.T., Haghani, A., Jourdain, E., Zoller, J.A., Li, C.Z., Steinman, K.J.,  
539 DiRocco, S., Schmitt, T., Osborn, S., Bonn, B.V., Katsumata, E., Mergl, J., Almunia, J.,  
540 Rodriguez, M., Haulena, M., Dold, C., and Horvath, S. 2021b. Multi-species and multi-  
541 tissue methylation clocks for age estimation in toothed whales and dolphins. *Commun.*  
542 *Biol.* **4**: 642.
- 543 Robeck, T.R., Haghani, A., Fei, Z., Lindemann, D.M., Russell, J., Herrick, K.E.S., Montano, G.,  
544 Steinman, K.J., Katsumata, E., Zoller, J.A., and Horvath, S. 2023. Multi-tissue DNA  
545 methylation aging clocks for sea lions, walruses, and seals. *Commun. Biol.* **6**: 359.
- 546 Sequeira, V., Neves, A., Vieira, A.R., Paiva, R.B., Canario, A., and Gordo, L.S. 2015.  
547 Estimating fecundity in the zygotarous species *Helicolenus dactylopterus*  
548 (Actinopterygii, Scorpaeniformes): adaptation of the gravimetric method. *Hydrobiologia.*  
549 **758**: 211–222.
- 550 Seutin, G., White, B.N., and Boag, P.T. 1991. Preservation of avian blood and tissue samples for  
551 DNA analyses. *Can. J. Zool.* **69**(1): 82–90.

- 552 Thompson, R.F., Atzmon, G., Cheorghhe, C., Liang, H.Q., Lowes, C., Grealley, J.M., and Barzilai,  
553 N. 2010. Tissue-specific dysregulation of DNA methylation in aging. *Aging Cell*. **9**(4):  
554 506–518.
- 555 Thompson, M.J., Chwialkowska, K., Rubbi, L., Lusi, A.J., Davis, R.C., Srivastava, A.,  
556 Korstanje, R., Churchill, G.A., Horvath, S., and Pellegrini, M. 2018. A multi-tissue full  
557 lifespan epigenetic clock for mice. *Aging*. **10**(10): 2832–2854.
- 558 Trucchi, E., Mazzarella, A.B., Gilfillan, G.D., Lorenzo, M.T., and Schonswetter, O.P. 2016.  
559 BsRADseq: screening DNA methylation in natural populations of non-model species.  
560 *Mol. Ecol.* **25**: 1697–1713.
- 561 van Buuren, S., and Groothuis-Oudshoorn, K. 2011. mice: Multivariate imputation by chained  
562 equations in R. *J. Stat. Softw.* **45**(3): 1–67.
- 563 Venney, C.J., Johansson, M.L., and Heath, D.D. 2016. Inbreeding effects on gene-specific DNA  
564 methylation among tissues of Chinook salmon. *Mol. Ecol.* **25**: 4521–4533.
- 565 Weber, D.N., Fields, A.T., Patterson III, W.F., Barnett, B.K., Hollenbeck, C.M., and Portnoy,  
566 D.S. 2022. Novel epigenetic age estimation in wild-caught Gulf of Mexico reef fishes.  
567 *Can. J. Fish. Aquat. Sci.* **79**: 1–5.
- 568 Yamagishi, G., Iguchi, T., and Miyagawa, S. 2022. Epigenetic regulation of sex determination  
569 and toxicity in non-mammalian vertebrates. *Genomic and Epigenomic Biomarkers of*  
570 *Toxicology and Disease: Clinical and Therapeutic Actions*, First Edition. pp 415–448.  
571 John Wiley & Sons, Ltd.
- 572 Yusipov, I., Bacalini, M.G., Kalyakulina, A., Krivonosov, M., Pirazzini, C., Gensous, N.,  
573 Ravaioli, F., Milazzo, M., Giuliani, C., Vedunova, M., Fiorito, G., Gagliardi, A.,  
574 Polidoro, S., Garagnani, P., Ivanchenko, M., and Franceschi, C. 2020. Age-related DNA

575 methylation changes are sex-specific: a comprehensive assessment. *Aging*. **12**(23):  
576 24057–24080.

577 Zupkovitz, G., Kabiljo, J., Kothmayer, M., Schlick, K., Schofer, C., Lagger, S., and Pusch, O.  
578 2021. Analysis of methylation dynamics reveals a tissue-specific, age-dependent decline  
579 in 5-methylcytosine within the genome of the vertebrate aging model *Nothobranchius*  
580 *furzeri*. *Front. Mol. Biosci.* **8**: 627143.

Draft

**Table 1.** Summary statistics for epigenetic clocks developed for the blackbelly rosefish using fin clips, muscle, and both tissue types combined, including the age range of fish in years, the number of CpG sites included in the model, the number individuals included in training and testing datasets, the coefficient of determination ( $R^2$ ), and the mean absolute error (MAE) reported in years.

<b>Model</b>	<b>Age range</b>	<b>CpG sites</b>	<b>Dataset</b>	<b>Individuals</b>	<b><math>R^2</math></b>	<b>MAE</b>
Fin clip	9–59	316	Training	44	0.98	1.66
			Testing	12	0.98	1.62
Muscle	9–60	312	Training	29	0.99	2.07
			Testing	8	0.98	2.14
<b>Multi-tissue</b>						
<i>Fin clip</i>	9–59	498	Training	44	0.93	2.94
			Testing	12	0.94	3.08
<i>Muscle</i>	9–60	498	Training	29	0.92	5.75
			Testing	8	0.77	5.43

**Table 2.** Summary statistics for epigenetic clocks developed with the inclusion of biological information (i.e., length and sex data), including the age range of fish in years, the number of CpG sites included in the model, the number individuals included in training and testing datasets, the coefficient of determination ( $R^2$ ), and the mean absolute error (MAE) reported in years.

Model	Age range	CpG sites	Dataset	Individuals	$R^2$	MAE
Fin clip	9–59	316	Training	44	0.98	1.66
			Testing	12	0.98	1.62
Fin clip + length	9–59	313	Training	44	0.99	1.47
			Testing	11	0.99	0.90
Fin clip + length by sex						
<i>Males</i>	9–37	448	Training	23	0.99	0.93
			Testing	6	0.99	0.43
<i>Females</i>	11–59	306	Training	20	0.99	1.26
			Testing	5	0.99	0.42
Muscle	9–60	312	Training	29	0.99	2.07
			Testing	8	0.98	2.14
Muscle + length	9–60	250	Training	29	0.99	2.12
			Testing	8	0.99	1.25
Muscle + length by sex						
<i>Males</i>	9–60	685	Training	13	0.99	1.16
			Testing	3	0.99	0.78
<i>Females</i>	13–60	489	Training	16	0.99	0.94
			Testing	4	0.99	0.80

**Table 3.** Index of average percent error (iAPE) for blackbelly rosefish epigenetic clock predicted age estimates versus consensus age estimates produced from paired-reader ages and eye lens core  $\Delta^{14}\text{C}$  values. Training dataset iAPE estimates were computed via leave-one-out, while test dataset iAPE values were produced from age predictions for samples not included in epigenetic clock development.

<b>Model</b>	<b>Training n</b>	<b>Training iAPE %</b>	<b>Testing n</b>	<b>Testing iAPE %</b>
Fin clip	44	4.46	12	2.77
Fin clip + length	44	3.86	11	2.09
Fin clip + length by sex	43	2.95	11	1.04
Muscle	29	5.23	8	4.31
Muscle + length	29	5.02	8	2.77
Muscle + length by sex	29	2.67	7	1.45

**Figure 1.** Digital image of a sagittal otolith section viewed with transmitted light from a 352 mm total length female blackbelly rosefish (N1307) with a consensus age estimate of 60 years.

**Figure 2.** Epigenetic age predictions versus consensus ages for epigenetic clocks developed using fin clip samples (A,B; red circles) and muscle tissue samples (C,D; blue circles). The lefthand panels depict the training datasets and righthand panels the testing datasets. Dashed lines indicate lines of 1:1 agreement between predicted and consensus ages. Solid lines represent linear regression fits to the data. The coefficient of determination ( $R^2$ ) and mean absolute error (MAE) reported in years are displayed on panels.

**Figure 3.** Epigenetic age predictions versus consensus ages for epigenetic clocks developed using fin clip samples (A,B; red circles) and muscle tissue samples (C,D; blue circles) with the inclusion of length data. The lefthand panels depict the training datasets and righthand panels the testing datasets. Dashed lines indicate lines of 1:1 agreement between predicted and consensus ages. Solid lines represent linear regression fits to the data. The coefficient of determination ( $R^2$ ) and mean absolute error (MAE) reported in years are displayed on panels.

**Figure 4.** Epigenetic age predictions versus consensus ages for epigenetic clocks developed using fin clip samples (A,B; red) and muscle tissue samples (C,D; blue) with the inclusion of length data and separately for males (depicted as squares) and females (depicted as circles). The lefthand panels depict the training datasets and righthand panels the testing datasets. Dashed lines indicate lines of 1:1 agreement between predicted and consensus ages. Solid lines represent linear regression fits to the data. The coefficient of determination ( $R^2$ ) and mean absolute error (MAE) reported in years are displayed on panels.

**Figure 5.** Epigenetic age predictions versus consensus ages for the multi-tissue epigenetic clock. Panel A depicts the training dataset and panel B depicts the testing dataset. Dashed lines indicate lines of 1:1 agreement between predicted and consensus ages. Solid lines represent linear regression fits to the data. The coefficient of determination ( $R^2$ ) and mean absolute error (MAE) reported in years are displayed on panels, with ‘FC’ indicating fin clips and ‘MU’ indicating muscle tissue.

Draft

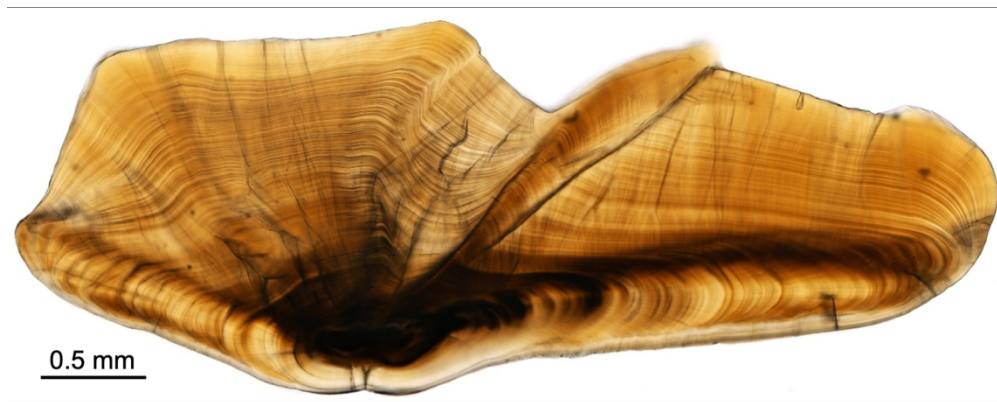


Figure 1. Digital image of a sagittal otolith section viewed with transmitted light from a 352 mm total length female blackbelly rosefish (N1307) with a consensus age estimate of 60 years.

165x65mm (300 x 300 DPI)

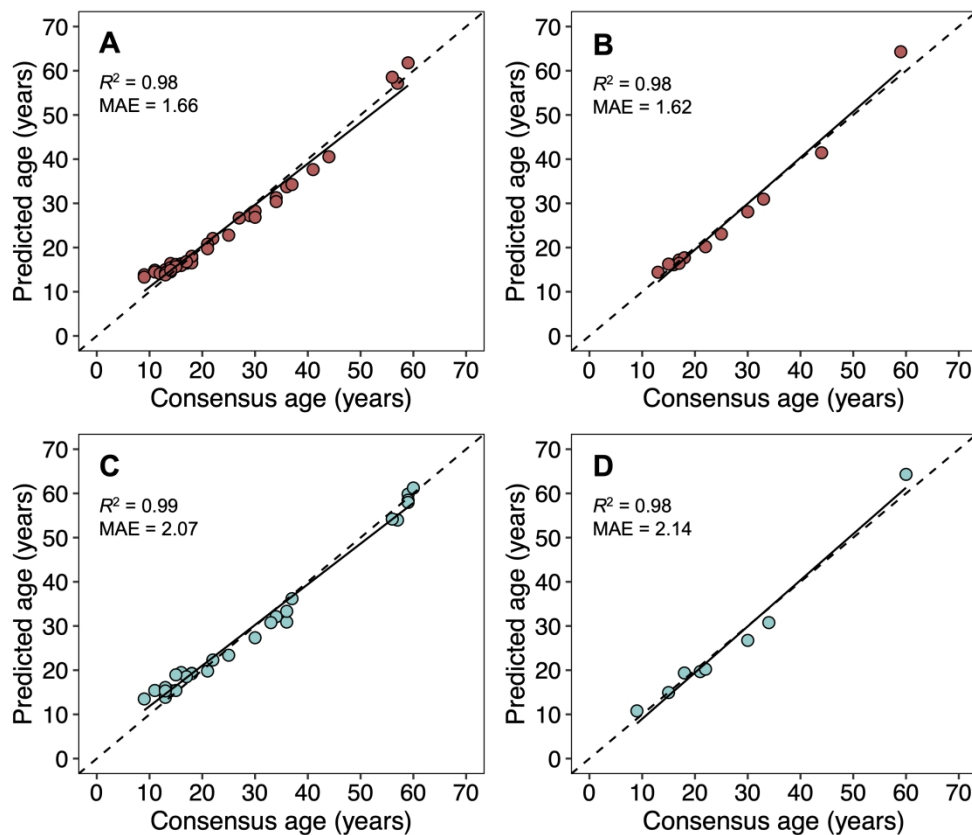


Figure 2. Epigenetic age predictions versus consensus ages for epigenetic clocks developed using fin clip samples (A,B; red circles) and muscle tissue samples (C,D; blue circles). The lefthand panels depict the training datasets and righthand panels the testing datasets. Dashed lines indicate lines of 1:1 agreement between predicted and consensus ages. Solid lines represent linear regression fits to the data. The coefficient of determination ( $R^2$ ) and mean absolute error (MAE) reported in years are displayed on panels.

1163x996mm (72 x 72 DPI)

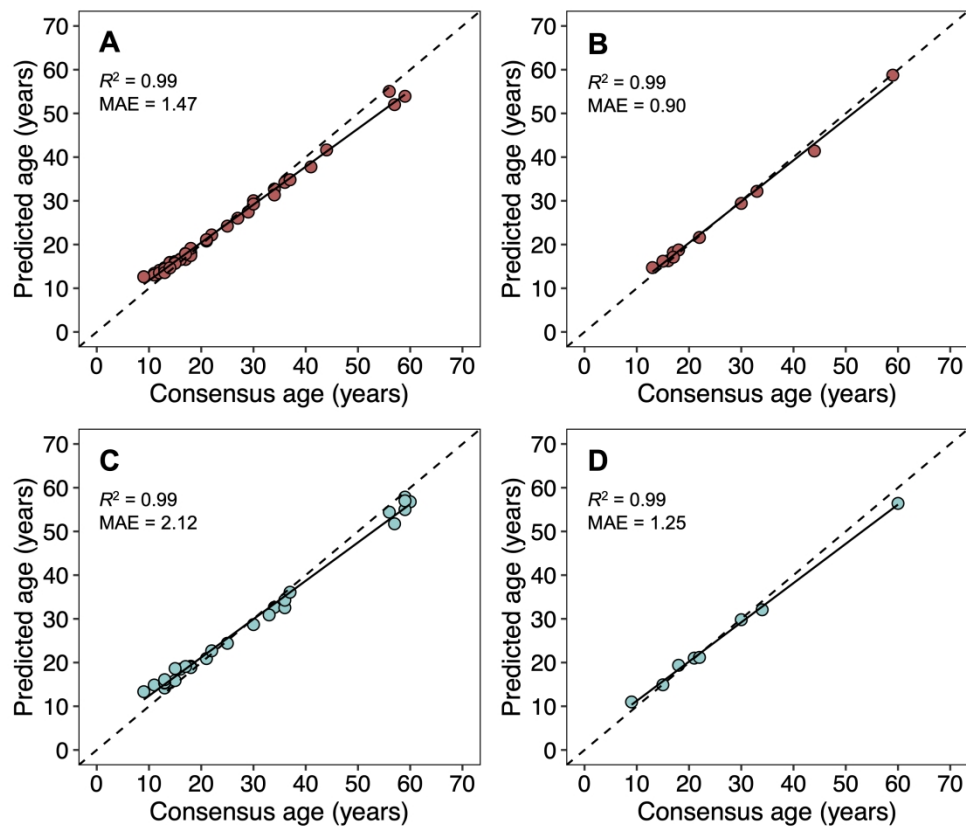


Figure 3. Epigenetic age predictions versus consensus ages for epigenetic clocks developed using fin clip samples (A,B; red circles) and muscle tissue samples (C,D; blue circles) with the inclusion of length data. The lefthand panels depict the training datasets and righthand panels the testing datasets. Dashed lines indicate lines of 1:1 agreement between predicted and consensus ages. Solid lines represent linear regression fits to the data. The coefficient of determination ( $R^2$ ) and mean absolute error (MAE) reported in years are displayed on panels.

1175x1009mm (72 x 72 DPI)

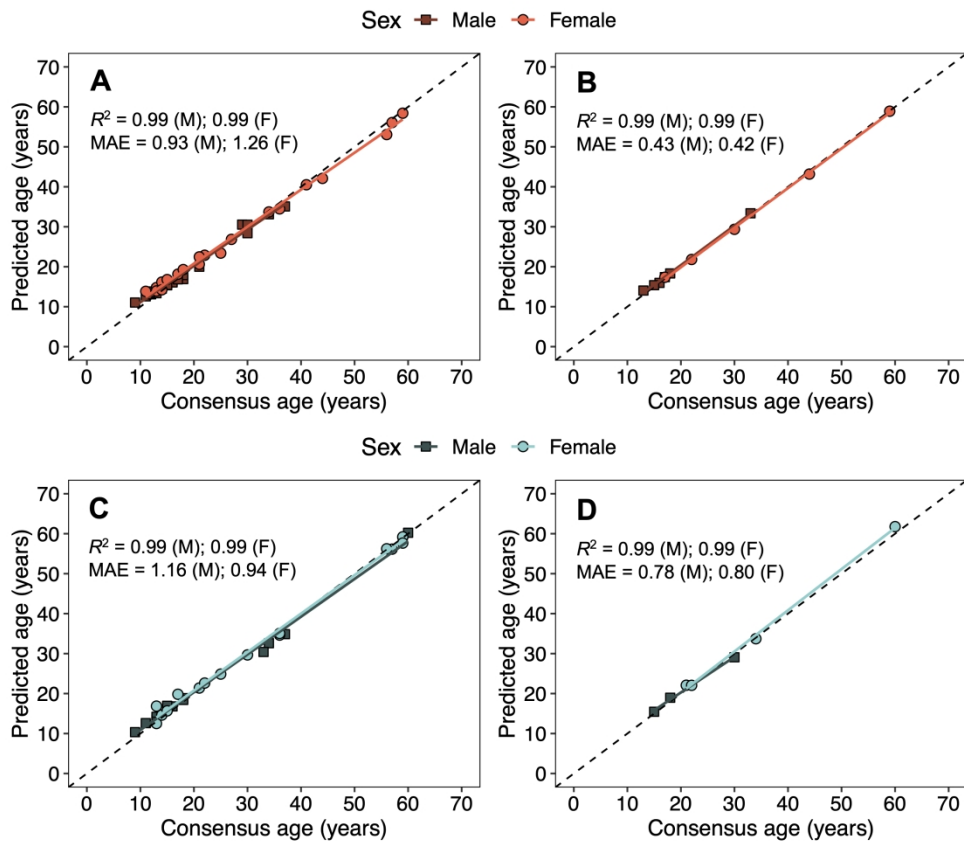


Figure 4. Epigenetic age predictions versus consensus ages for epigenetic clocks developed using fin clip samples (A,B; red) and muscle tissue samples (C,D; blue) with the inclusion of length data and separately for males (depicted as squares) and females (depicted as circles). The lefthand panels depict the training datasets and righthand panels the testing datasets. Dashed lines indicate lines of 1:1 agreement between predicted and consensus ages. Solid lines represent linear regression fits to the data. The coefficient of determination ( $R^2$ ) and mean absolute error (MAE) reported in years are displayed on panels.

1177x1032mm (72 x 72 DPI)

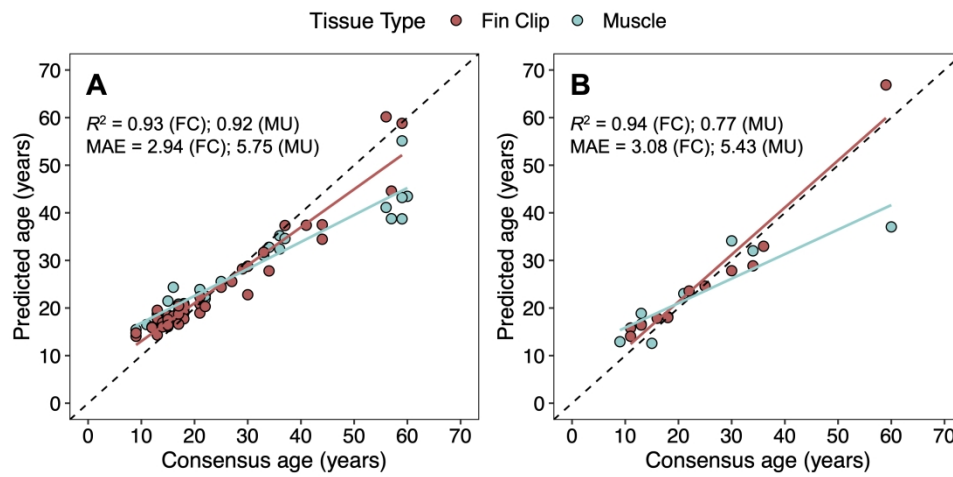


Figure 5. Epigenetic age predictions versus consensus ages for the multi-tissue epigenetic clock. Panel A depicts the training dataset and panel B depicts the testing dataset. Dashed lines indicate lines of 1:1 agreement between predicted and consensus ages. Solid lines represent linear regression fits to the data. The coefficient of determination ( $R^2$ ) and mean absolute error (MAE) reported in years are displayed on panels, with 'FC' indicating fin clips and 'MU' indicating muscle tissue.

1184x599mm (72 x 72 DPI)